

# Tensor network approach to phase transitions of a non-Abelian topological phase

Wen-Tao Xu<sup>1</sup>, Qi Zhang<sup>1</sup> and Guang-Ming Zhang<sup>1,2</sup>

<sup>1</sup>State Key Laboratory of Low-Dimensional Quantum Physics and  
Department of Physics, Tsinghua University, Beijing 100084, China

<sup>2</sup>Frontier Science Center for Quantum Information, Beijing 100084, China.

(Dated: March 3, 2022)

The non-abelian topological phase with Fibonacci anyons minimally supports universal quantum computation. In order to investigate the possible phase transitions out of the Fibonacci topological phase, we propose a generic quantum-net wavefunction with two tuning parameters dual with each other, and the norm can be exactly mapped into a partition function of the two-coupled  $\phi^2$ -state Potts models, where  $\phi = (\sqrt{5} + 1)/2$  is the golden ratio. By developing the tensor network representation of this wavefunction on a square lattice, we can accurately calculate the full phase diagram with the numerical methods of tensor networks. More importantly, it is found that the non-abelian Fibonacci topological phase is enclosed by three distinct non-topological phases and their dual phases of a single  $\phi^2$ -state Potts model: the gapped dilute net phase, critical dense net phase, and spontaneous translation symmetry breaking gapped phase. We also determine the critical properties of the phase transitions among the Fibonacci topological phase and those non-topological phases.

*Introduction.* - In recent years theoretical and experimental search for topological quantum phases of matter with anyonic excitations have attracted considerable attention, because non-abelian quasiparticles are necessary ingredient for topological quantum computation[1–5]. Since the non-abelian topological phases are characterized by fractionalized degrees of freedom[3, 6], the Landau-Ginzburg-Wilson theory cannot be used to characterize these exotic phases, and their phase transition to other non-topological phases is an important open problem.

One remarkable feature of topological phases is that the ground-state wave function encodes many of the quasiparticle properties, which was exploited as far back as the Laughlin’s pioneering work on fractional quantum Hall effect[7]. Many properties of the topological phases can also be deduced by mapping the wavefunction to a statistical mechanics model. In this paper, we will develop a tensor network approach by constructing a generic topological wavefunction with tuning parameters, which directly encodes the topological properties in the virtual symmetries of the local tensor. By studying the corresponding partition function, we can detect possible topological phase transitions and identify the associated anyon-condensation mechanism.

The Fibonacci anyon phase is the simplest one supporting universal quantum computation. The Fibonacci anyon  $\tau$  obeys the non-abelian fusion rule:  $\tau \otimes \tau = 1 \oplus \tau$ , where 1 is the trivial particle, and one Fibonacci anyon carries a non-integer quantum dimension  $\phi = (\sqrt{5} + 1)/2$ . A prototype lattice model realizing the Fibonacci anyons is the Levin-Wen string-net model[8] with additional two types of anyons:  $\bar{\tau}$  with the opposite chirality to  $\tau$  and a bosonic composite particle  $b = \tau \otimes \bar{\tau}$ . This string-net model just represents the fixed point of the doubled Fibonacci (DFib) topological phase with zero correlation length. To consider the topological phase transitions out

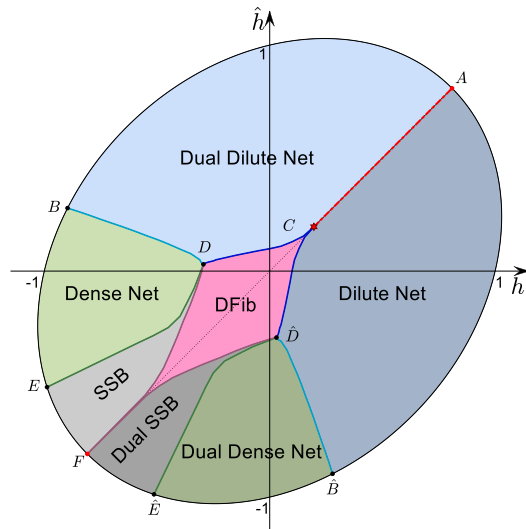


FIG. 1: The global phase diagram for the generic quantum-net phase with two dual parameters. The phase diagram is symmetric about the self-dual line  $h = \hat{h}$  and bounded by the elliptic curve of the two-decoupled Potts models. The  $AC$  dot-dashed line represents a weak first-order transition and all other solid lines are continuous transitions.  $C$  denotes a tri-critical point and  $D$  is a tetra-critical point.

of the DFib topological phase, one has to drive the string-net model away from its fixed point by introducing a string tension[9–12]. However, due to the lack of quantum self-duality, a generic phase diagram of the DFib topological phase has not been obtained.

It was noticed that a quantum-net model is suggested to describe the DFib topological order with a finite correlation length on a square lattice[13, 14]. The most important feature is the presence of quantum self-duality. In this paper, we propose a generic DFib quantum-net wavefunction with *two* dual string tensions[15], and its

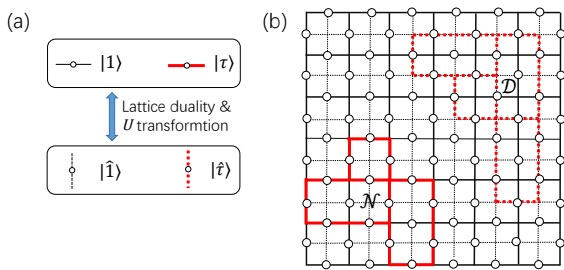


FIG. 2: (a) Two local orthogonal quantum states  $|1\rangle$  and  $|\tau\rangle$  and their dual local states  $|\hat{1}\rangle$  and  $|\hat{\tau}\rangle$ . (b) The physical degrees of freedom locate at the edges of the square lattice. The full lines denote the original lattice while the dash lines are dual lattice.  $\mathcal{N}$  and  $\mathcal{D}$  are two typical nets.

norm can be mapped into a partition function of the two-coupled  $\phi^2$ -state Potts models, whose Boltzmann weights can be negative. In order to study the quantum topological phase transitions numerically, we derive the triple-line tensor network state (TNS) representation of this generic wavefunction. Then the global phase diagram is fully established using the corner transfer matrix (CTM) method[16–19] and variational uniform matrix product state (VUMPS) method[19–21]. As shown in Fig. 1, the non-abelian DFib phase is present only in the two-coupled Potts models and surrounded by three distinct non-topological phases and their dual phases: the gapped dilute net phase, critical dense net phase, and spontaneous symmetry breaking (SSB) gapped phase.

*Generic quantum-net wavefunction.* - The quantum-net wavefunction involves nets and chromatic polynomials[14]. An edge of the lattice is either empty or occupied by  $\tau$  string, yielding two mutually orthogonal quantum states  $|1\rangle$  and  $|\tau\rangle$ , see Fig. 2 (a). A  $\tau$  string consists of the  $|\tau\rangle$  states on the connected edges, and a net  $\mathcal{N}$  is formed by the closed  $\tau$  strings which are allowed to branch and cross, as shown in Fig. 2 (b). Since the net  $\mathcal{N}$  divides the two-dimensional manifold into different regions, the chromatic polynomial  $\chi_{\mathcal{N}}(Q)$  with  $Q \in \mathbb{N}_+$  counts the ways of coloring the net  $\mathcal{N}$  using  $Q$  different colors (nets  $\mathcal{N}$  and  $\hat{\mathcal{N}}$  are dual each other), such that the neighboring regions sharing a boundary are colored differently. Since  $\chi_{\mathcal{N}}(Q)$  is a polynomial of  $Q$ , it can be generalized to  $Q \in \mathbb{R}$ .

On a square lattice, the DFib quantum-net wave function[13, 14] is given by the superposition of nets  $\mathcal{N}$ :

$$|\Psi\rangle = \sum_{\mathcal{N}} \phi^{-L_{\mathcal{N}}/2} \chi_{\mathcal{N}}(\phi^2) |\mathcal{N}\rangle, \quad (1)$$

where  $L_{\mathcal{N}}$  is the total length of the  $\tau$  strings in the net  $\mathcal{N}$  and  $\phi^{-L_{\mathcal{N}}/2}$  is viewed as a string tension. The end of  $\tau$  string will carry a Fibonacci anyon with fractionalized quantum dimension  $\phi$ . To show the quantum self-duality, the wave function  $|\Psi\rangle$  has to be written on the dual lattice in terms of the orthogonal quantum states  $|\hat{1}\rangle$  and  $|\hat{\tau}\rangle$ ,

which are related to the local states  $|1\rangle$  and  $|\tau\rangle$  via the transformation[13]:

$$U = \begin{pmatrix} \langle 1|\hat{1}\rangle & \langle \tau|\hat{1}\rangle \\ \langle 1|\hat{\tau}\rangle & \langle \tau|\hat{\tau}\rangle \end{pmatrix} = \frac{1}{\phi} \begin{pmatrix} 1 & \sqrt{\phi} \\ \sqrt{\phi} & -1 \end{pmatrix}. \quad (2)$$

Then the dual quantum-net wavefunction has the same form as  $|\Psi\rangle$ .

Inspired by the deformed  $\mathbb{Z}_2$  abelian topological phase[22, 23], we propose a generic quantum-net wavefunction

$$|\Psi(h, \hat{h})\rangle = \prod_{\text{edges}} P(h, \hat{h}) |\Psi\rangle, \quad (3)$$

where  $P(h, \hat{h}) = (1 + h\sigma^z + \hat{h}\hat{\sigma}^z)$  is the deformation matrix acting on all edges,  $\sigma^z$  is the diagonal Pauli matrix in the  $|1\rangle$  and  $|\tau\rangle$  basis, and  $\hat{\sigma}^z = U\sigma^z U^{-1}$  is diagonal Pauli matrix in the  $|\hat{1}\rangle$  and  $|\hat{\tau}\rangle$  basis.  $h$  and  $\hat{h}$  describe the string tensions. The quantum duality transforms  $|\Psi(h, \hat{h})\rangle$  into  $|\Psi(\hat{h}, h)\rangle$ , and the quantum self-duality exhibits when  $h = \hat{h}$ .

It should be emphasized that the generic wavefunction still has a local parent Hamiltonian. As it is shown, the quantum-net  $|\Psi\rangle$  has a frustration-free parent Hamiltonian:  $H = \sum_a H_a$  is a sum of local positive projectors [14]. Since the deformation matrix  $P$  is a local positive definite operators, the parent Hamiltonian of the generic wavefunction is given by  $H(h, \hat{h}) = \sum_a P_a^{-1} H_a P_a^{-1}$ , where  $P_a$  is a product of  $P$  in the support of  $H_a$ . The possible quantum critical points of this parent Hamiltonian are characterized by the so-called conformal quantum critical points[24, 25], where all equal-time correlators of local operators are described by two-dimensional conformal field theories (CFTs).

*Mapping to two-coupled Potts models.* - To extract the possible quantum phase transitions out of the DFib topological phase, we consider the norm of the generic quantum-net wavefunction,

$$\mathcal{Z} = \sum_{\mathcal{N}, \mathcal{N}'} \chi_{\mathcal{N}}(\phi^2) \chi_{\mathcal{N}'}(\phi^2) \prod_{\text{edge}} W_{n, n'}, \quad (4)$$

where  $\mathcal{N}$  and  $\mathcal{N}'$  denote the nets in the bra and ket layers and  $n, n' = 1$  or  $\tau$  corresponds to the empty or  $\tau$ -string occupied edge. The weight matrix  $W$  is given by

$$W = W_0 \begin{pmatrix} 1 & e^{-K} \\ e^{-K} & e^{-2K-K'} \end{pmatrix}, \quad (5)$$

where

$$e^{-K} = \frac{4\hat{h}/\phi^2}{4\hat{h}^2/\phi^3 + (1 + h - \hat{h}/\phi^3)^2},$$

$$e^{-K'} = \frac{4\hat{h}^2/\phi^3 + (1 - h + \hat{h}/\phi^3)^2}{4\hat{h}^2/\phi^2 + \phi(1 + h - \hat{h}/\phi^3)^2} e^{2K}. \quad (6)$$

Since the  $Q$ -state Potts model is expressed as  $\mathcal{Z}_{\text{Potts}} = \sum_{\mathcal{N}} e^{-\beta L_{\mathcal{N}}} \chi_{\mathcal{N}}(Q)$ ,  $e^{-K}$  can be viewed as the Boltzmann weight for the  $\phi^2$ -state Potts model, while  $K'$  describes the inter-layer coupling. Therefore, instead of the previous  $(\phi+2)$ -state Potts model[26], the wavefunction norm (4) is mapped into the partition function of two-coupled  $\phi^2$ -state Potts models. Such a statistical model is unusual in the sense that it involves negative Boltzmann weight in the parameter region ( $\hat{h} < 0$ ). However, the appearance of such minus forms pairs and will not spoil the solution to the partition function.

Numerous exact results can be deduced. When the coupling of the two  $\phi^2$ -state Potts models vanishes, the deformation matrix  $P(h, \hat{h})$  just projects out the trivial product states[23], i.e.,  $\det P(h, \hat{h}) = 0$ , corresponding to an elliptic equation  $h^2 - 2h\hat{h}/\phi^3 + \hat{h}^2 = 1$  as the boundary of the phase diagram (Fig. 1). From this equation, we can find two self-dual points  $h = \hat{h} = \pm\phi/2$ . One is identified as the ferromagnetic critical point  $A$  separating the gapped dilute net phase and its dual phase[27], and the other was considered as an "unphysical" point  $F$  in the previous study[28]. However, we will use the TNS methods to show that the point  $F$  is a multi-critical point, around which a new phase with translational symmetry breaking and its dual phase are found[29].

Along the self-dual line  $h = \hat{h}$ , it has been known that the transfer operators of the two-coupled Potts models are endowed with  $SO(4)_3$  Birman-Murakami-Wenzl algebra and a critical point  $C \approx (0.197, 0.197)$  has been found by the level-rank duality[30], which is described by the coset CFT with a central charge  $c = 27/20$ . As shown in Fig. 1, this critical point  $C$  divides the self-dual line into two parts: the DFib topological part  $CF$  and the first-order phase transition line  $AC$  between the dilute net phase and its dual phase[29].

*Tensor network representation.* - In order to explore the large parameter space of the global phase diagram, we have to employ the numerical calculations. Before that, the TNS representation of the generic quantum-net wavefunction should be established. Since the non-local chromatic polynomials are involved in the wavefunction, auxiliary degrees of freedom on the dual vertices are introduced to express the wavefunction in terms of local structures. It is known that the TNS representation of the Levin-Wen Fibonacci string-net  $|\Psi_{\text{SN}}\rangle$  on the honeycomb lattice has been established[31, 32]. When each vertex of a square lattice is split into two and added new edges with no physical degrees of freedom, the square lattice is transformed into the honeycomb lattice. Taking the advantage of the deletion-contraction relation[13] displayed Fig. 3 (a), we can obtain the corresponding chromatic polynomial on the square lattice so that the TNS for the quantum-net can be constructed.

As shown in Figs. 3 (b) and (c), the local tensor of the quantum-net on the square lattice is derived by con-

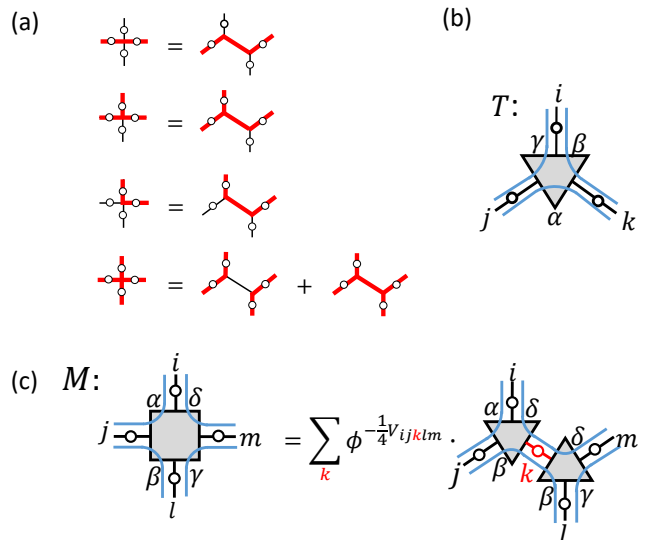


FIG. 3: (a) The square lattice is transformed to a honeycomb lattice. (b) The triple line local tensor  $T$  in the string-net wavefunction. (c) Contracting two tensors  $T$  yields the tensor  $M$  on the square lattice.

tracting two triple-line tensors  $T_{\beta\delta\alpha}^{ijk}$  via

$$M_{\alpha\beta\gamma\delta}^{ijlm} = \sum_k \phi^{-V_{ijklm}/4} T_{\beta\delta\alpha}^{ijk} T_{\delta\beta\gamma}^{lmk},$$

$$V_{ijklm} = 3\delta_{k\tau}(\delta_{i\tau}\delta_{j\tau} + \delta_{l\tau}\delta_{m\tau}) + \delta_{i\tau} + \delta_{j\tau} + \delta_{l\tau} + \delta_{m\tau}.$$

Then the TNS of the quantum-net wavefunction is expressed as

$$|\Psi\rangle = \sum_{\{\dots ijlm \dots\}} \text{tTr} \left[ \bigotimes_{\text{vertex}} M_{\alpha\beta\gamma\delta}^{ijlm} \right] |\dots ijlm \dots\rangle, \quad (7)$$

where "tTr" denotes the tensor contraction over all auxiliary indices. Finally, the deformed DFib quantum-net wavefunction  $|\Psi(h, \hat{h})\rangle$  is derived with the modified local tensor  $\widetilde{M}_{\alpha\beta\gamma\delta}^{ijlm}$ , which can be obtained by acting the deformation matrix  $P$  on the physical indices of  $M_{\alpha\beta\gamma\delta}^{ijlm}$ .

In the TNS representation, the topologically degenerated ground state can be characterized with matrix product operators (MPOs) acting on the auxiliary degrees of freedom[33–35]. The quantum-net  $|\Psi(h, \hat{h})\rangle$  shares the same MPOs as those of the Fibonacci string-net, and the MPOs are independent of the deformation parameters  $h$  and  $\hat{h}$ . On a torus, the degenerate ground state space is spanned by four minimal entangled states[36] labelled as  $|\mathbf{1}\rangle$ ,  $|\boldsymbol{\tau}\rangle$ ,  $|\bar{\boldsymbol{\tau}}\rangle$  and  $|\mathbf{b}\rangle$ . With the MPO algebra[12, 33], it can be checked that our generic wavefunction  $|\Psi(h, \hat{h})\rangle = |\mathbf{1}\rangle + |\mathbf{b}\rangle$ . By inserting MPOs winding around the TNS wavefunction  $|\Psi(h, \hat{h})\rangle$ , other three linear combinations of the minimal entangled states can be obtained. In the generic TNSs, the well-defined anyonic excitations can be created by simply manipulating on the auxiliary degrees of freedom with MPOs, so one can easily measure

the condensation and confinement of anyons[34, 37]. To probe the quantum phase transitions, it is sufficient to focus on  $|\Psi(h, \hat{h})\rangle$  without MPO insertion. However, if one concerns about the fates of  $\tau$  and  $\bar{\tau}$  anyons, the TNSs with the MPO insertions[38] must be taken into consideration. Furthermore, the MPO symmetry of the local tensor also constrains the possible CFTs describing conformal critical points[39, 40], and the CFTs must contain a quantum dimension  $\phi^2$ .

*Global phase diagram.* - With the TNS for the deformed quantum net at hand, those TNS algorithms can be applied. Integrating the physical variables of the generic DFib wavefunction yields the partition function in the form of a double-layer tensor network

$$\mathcal{Z} = \text{tTr} \left( \bigotimes_{\text{vertex}} \mathbb{M} \right) = \text{Tr}(\mathbb{T}^{L_x}), \quad (8)$$

where  $\mathbb{M}$  is the local double triplet-line tensor obtained by contracting the physical indices of  $\bar{M}$  and its conjugate,  $\mathbb{T}$  is the column-to-column transfer operator, and  $L_x$  is the number of columns. In order to determine the various phase boundaries, we need to calculate the correlation length, whose divergent peaks give rise to the position of the continuous phase transitions. When the transfer operator  $\mathbb{T}$  is hermitian, we employ the VUMPS[19–21] to extract the correlation length, while for non-hermitian  $\mathbb{T}$  in the lower half-plane of Fig.1, the CTM[16–19] method is used.

Along the axis of  $h$ , the numerical TNS calculation with VUMPS algorithm has been performed with large bond dimensions  $D = 80, 100, 120$ . As shown in Fig. 4 (a), there is a phase transition from the DFib topological phase to the dilute net phase around  $h \approx 0.1$ . The peak position of the correlation length is nearly the same for different bond dimensions. The corresponding phase transition is still described by the CFT with a central charge  $c = 14/15$ , similar to that of the deformed DFib string-net[12]. As  $h$  is further increasing, the correlation length first shows a divergent peak around  $h \approx -0.3$  and then appears a hump, which gradually becomes a broad peak with increasing the bond dimension. After this hump, the system enters into a gapless dense net phase. The finite entanglement scaling Fig. 4 (c) suggests that the dense net phase is described by the CFT with central charge  $c = 7/5$ , corresponding to the squared tri-critical Ising universality class. Between the DFib topological phase and the dense net phase, we find a narrow region of the gapped phase with translational symmetry breaking. In order to clearly see the SSB phase, we display the correlation length along the cut  $\hat{h} = -0.8 - h$  in Fig. 4 (b), where the CTM methods are employed with the bond dimensions  $D = 45, 55$ . The SSB phase exists between the two peaks of the correlation length.

Moreover, the critical line  $BD$  separating the dense net phase and dual dilute net phase terminates at a special

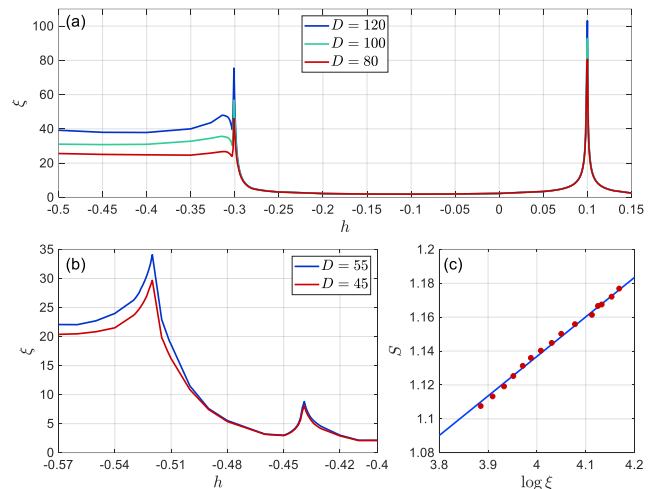


FIG. 4: (a) The correlation length  $\xi$  obtained by the VUMPS method with bond dimensions  $D$  along  $h$  axis of the phase diagram. (b) The correlation length deduced from the CTM method with bond dimensions  $D$  along the cut  $\hat{h} = -0.8 - h$ .  $h = -0.4$  sits on the self-dual line. (c) The entanglement entropy  $S$  at the point  $(h, \hat{h}) = (-0.6, 0)$ . The blue line is  $S = \frac{c}{6} \log \xi + S_0$  with the central charge  $c = 7/5$ .

point  $B = (-\sqrt{3-\phi} - 1/\phi, \sqrt{3-\phi} - 1/\phi)/2$ , which is the critical point of the decoupled antiferromagnetic  $\phi^2$ -state Potts models characterizing by two copies of  $\mathbb{Z}_3$  parafermion CFT with  $c = 8/5$  (Ref. [28]). But our numerics[29] shows that the full line  $BD$  is described by the CFT with the central charge  $c \simeq 1.4$ , as the same as the dense net phase. On the other hand, the critical line  $ED$  separating the dense net phase from the SSB phase is described by the CFT with the central charge  $c \simeq 1.6$ , while the continuous phase transition line  $FD$  between the DFib topological phase and the SSB phase is characterized by the CFT with a central charge  $c \approx 1.4$ . Four critical lines meet at a tetra-critical point  $D \approx (-0.294, 0.03)$ . Using the quantum duality, the complete phase diagram Fig. 1 is thus fully established.

The universal feature of all gapped phases is the degeneracies of dominant eigenvalues of the transfer operators with periodic boundary condition. Since  $|\Psi\rangle = |\mathbf{1}\rangle + |\mathbf{b}\rangle$ , the 2-fold degenerate dominant eigenvalues of the DFib topological phase correspond to  $\langle \mathbf{1}|\mathbf{1}\rangle$  and  $\langle \mathbf{b}|\mathbf{b}\rangle$ . Because  $b$  anyons are condensed in the dilute net phase, the 4-fold degenerate eigenvectors belong to the topological sectors  $\langle \mathbf{1}|\mathbf{1}\rangle$ ,  $\langle \mathbf{b}|\mathbf{b}\rangle$ ,  $\langle \mathbf{1}|\mathbf{b}\rangle$  and  $\langle \mathbf{b}|\mathbf{1}\rangle$ . In the dense net phase, however, the large nets dominate and  $b$  anyons are logarithmically confined. Due to the translation symmetry breaking in the SSB phase, there are two dominant eigenvectors with the momenta 0 and  $\pi$  for each bra and ket of the topological sectors, leading to 16-fold degeneracy. All these results have been confirmed in our numerical results[29].

*Conclusion.* - We have fully studied the non-abelian topological phase transitions out of a generic DFib topological state. The norm of the wave function is mapped into the partition function of the two-coupled  $\phi^2$ -state Potts models. With the tensor network representation and numerical TNS methods, a global phase diagram has been fully established. Previously we showed that[23] the  $Z_2$  toric code topological phase corresponds to the partial order phase of the Ashkin-Teller model – two-coupled Ising models. Here we further prove that the non-abelian DFib topological phase can be mapped to an inter-layer ordered phase of the two-coupled  $\phi^2$ -state Potts models, instead of the the previous  $(\phi + 2)$ -state Potts model[26].

Compared to the Hamiltonian approach, such a wavefunction approach has many advantages in applying the TNS methods to the quantum topological phase transitions among intrinsic topological phases. A natural question is how the conformal quantum criticality will be changed when the dynamics of the parent Hamiltonian for the generic DFib topological phase is considered. The related problems are under further investigations.

*Acknowledgment.*- The authors would like to thank Hai-Jun Liao for his providing the program of CTM algorithm and Guo-Yi Zhu for his stimulating discussions. The research is supported by the National Key Research and Development Program of MOST of China (2016YFYA0300300 and 2017YFA0302902).

- 
- [1] A. Y. Kitaev, *Annals of Physics* **303**, 2 (2003), URL <http://www.sciencedirect.com/science/article/pii/S0003491602000180>.
- [2] M. H. Freedman, *Communications in Mathematical Physics* **234**, 129 (2003).
- [3] A. Kitaev, *Annals of Physics* **321**, 2 (2006), ISSN 0003-4916, URL <http://www.sciencedirect.com/science/article/pii/S0003491605002381>.
- [4] C. Nayak, S. H. Simon, A. Stern, M. Freedman, and S. Das Sarma, *Rev. Mod. Phys.* **80**, 1083 (2008), URL <https://link.aps.org/doi/10.1103/RevModPhys.80.1083>.
- [5] X.-G. Wen, *Science* **363** (2019), URL <https://science.sciencemag.org/content/363/6429/eaal3099>.
- [6] X. Chen, Z.-C. Gu, and X.-G. Wen, *Phys. Rev. B* **82**, 155138 (2010), URL <https://link.aps.org/doi/10.1103/PhysRevB.82.155138>.
- [7] R. B. Laughlin, *Phys. Rev. Lett.* **50**, 1395 (1983), URL <https://link.aps.org/doi/10.1103/PhysRevLett.50.1395>.
- [8] M. A. Levin and X.-G. Wen, *Physical Review B* **71** (2005), URL <https://link.aps.org/doi/10.1103/PhysRevB.71.045110>.
- [9] M. D. Schulz, S. Dusuel, K. P. Schmidt, and J. Vidal, *Phys. Rev. Lett.* **110**, 147203 (2013), URL <https://link.aps.org/doi/10.1103/PhysRevLett.110.147203>.
- [10] S. Dusuel and J. Vidal, *Phys. Rev. B* **92**, 125150 (2015), URL <https://link.aps.org/doi/10.1103/PhysRevB.92.125150>.
- [11] A. Schotte, J. Carrasco, J. Haegeman, L. Vanderstraeten, F. Verstraete, and J. Vidal, arXiv:1909.06284 (2019), URL <http://arxiv.org/abs/1909.06284>.
- [12] M. Mariën, J. Haegeman, P. Fendley, and F. Verstraete, *Phys. Rev. B* **96**, 155127 (2017), URL <https://link.aps.org/doi/10.1103/PhysRevB.96.155127>.
- [13] P. Fendley, *Annals of Physics* **323**, 3113 (2008), URL <http://linkinghub.elsevier.com/retrieve/pii/S0003491608000614>.
- [14] P. Fendley, S. V. Isakov, and M. Troyer, *Physical Review Letters* **110** (2013), URL <https://link.aps.org/doi/10.1103/PhysRevLett.110.260408>.
- [15] W.-T. Xu and G.-M. Zhang, arXiv e-prints (unpublished), arXiv:1905.09960 (2019).
- [16] T. Nishino and K. Okunishi, *Journal of the Physical Society of Japan* **65**, 891 (1996), URL <https://doi.org/10.1143/JPSJ.65.891>.
- [17] R. Orús and G. Vidal, *Phys. Rev. B* **80**, 094403 (2009), URL <https://link.aps.org/doi/10.1103/PhysRevB.80.094403>.
- [18] P. Corboz, T. M. Rice, and M. Troyer, *Phys. Rev. Lett.* **113**, 046402 (2014), URL <https://link.aps.org/doi/10.1103/PhysRevLett.113.046402>.
- [19] M. T. Fishman, L. Vanderstraeten, V. Zauner-Stauber, J. Haegeman, and F. Verstraete, *Phys. Rev. B* **98**, 235148 (2018), URL <https://link.aps.org/doi/10.1103/PhysRevB.98.235148>.
- [20] L. Vanderstraeten, J. Haegeman, and F. Verstraete, *SciPost Phys. Lect. Notes* p. 7 (2019), URL <https://scipost.org/10.21468/SciPostPhysLectNotes.7>.
- [21] V. Zauner-Stauber, L. Vanderstraeten, M. T. Fishman, F. Verstraete, and J. Haegeman, *Physical Review B* **97** (2018), URL <https://link.aps.org/doi/10.1103/PhysRevB.97.045145>.
- [22] J. Haegeman, K. Van Acoleyen, N. Schuch, J. I. Cirac, and F. Verstraete, *Phys. Rev. X* **5**, 011024 (2015), URL <https://link.aps.org/doi/10.1103/PhysRevX.5.011024>.
- [23] G.-Y. Zhu and G.-M. Zhang, *Phys. Rev. Lett.* **122**, 176401 (2019), URL <https://link.aps.org/doi/10.1103/PhysRevLett.122.176401>.
- [24] E. Ardonne, P. Fendley, and E. Fradkin, *Annals of Physics* **310**, 493 (2004), URL <http://linkinghub.elsevier.com/retrieve/pii/S0003491604000247>.
- [25] C. Castelnovo, S. Trebst, and M. Troyer, arXiv:0912.3272 (2009), URL <http://arxiv.org/abs/0912.3272>.
- [26] L. Fidkowski, M. Freedman, C. Nayak, K. Walker, and Z. Wang, *Commun. Math. Phys.* **287**, 805 (2009), URL <https://doi.org/10.1007/s00220-009-0757-9>.
- [27] H. Saleur, *Nuclear Physics B* **360**, 219 (1991), URL <http://www.sciencedirect.com/science/article/pii/055032139190402J>.
- [28] J. L. Jacobsen and H. Saleur, *Nuclear Physics B* **743**, 207 (2006), URL <http://www.sciencedirect.com/science/article/pii/S0550321306001726>.
- [29] See the details in the Supplementary Materials.
- [30] P. Fendley and J. L. Jacobsen, *Journal of Physics A: Mathematical and Theoretical* **41**, 215001 (2008), URL <http://stacks.iop.org/1751-8121/41/i=21/a=215001?key=crossref.b622c38a08a1779c8dd3baf71daf5bba>.
- [31] Z.-C. Gu, M. Levin, B. Swingle, and X.-G. Wen, *Physical Review B* **79** (2009), URL <https://link.aps.org/doi/10.1103/PhysRevB.79.085118>.

- [32] O. Buerschaper, M. Aguado, and G. Vidal, Physical Review B **79** (2009), URL <https://link.aps.org/doi/10.1103/PhysRevB.79.085119>.
- [33] N. Bultinck, M. Mariën, D. J. Williamson, M. B. Şahinoğlu, J. Haegeman, and F. Verstraete, Annals of Physics **378**, 183 (2017), URL <http://www.sciencedirect.com/science/article/pii/S0003491617300040>.
- [34] N. Schuch, D. Poilblanc, J. I. Cirac, and D. Pérez-García, Phys. Rev. Lett. **111**, 090501 (2013), URL <https://link.aps.org/doi/10.1103/PhysRevLett.111.090501>.
- [35] N. Schuch, I. Cirac, and D. Pérez-García, Annals of Physics **325**, 2153 (2010), URL <http://www.sciencedirect.com/science/article/pii/S0003491610000990>.
- [36] Y. Zhang, T. Grover, A. Turner, M. Oshikawa, and A. Vishwanath, Phys. Rev. B **85**, 235151 (2012), URL <https://link.aps.org/doi/10.1103/PhysRevB.85.235151>.
- [37] J. Haegeman, V. Zauner, N. Schuch, and F. Verstraete, Nature Communications **6**, 8 (2015), ISSN 2041-1723, URL <http://dx.doi.org/10.1038/ncomms9284>.
- [38] R. Vanhove, M. Bal, D. J. Williamson, N. Bultinck, J. Haegeman, and F. Verstraete, Phys. Rev. Lett. **121**, 177203 (2018), URL <https://link.aps.org/doi/10.1103/PhysRevLett.121.177203>.
- [39] M. Buican and A. Gromov, Communications in Mathematical Physics **356**, 1017 (2017), ISSN 1432-0916, URL <https://doi.org/10.1007/s00220-017-2995-6>.
- [40] C. Gils, E. Ardonne, S. Trebst, D. A. Huse, A. W. W. Ludwig, M. Troyer, and Z. Wang, Phys. Rev. B **87**, 235120 (2013), URL <https://link.aps.org/doi/10.1103/PhysRevB.87.235120>.